Biophysical Chemistry 180–181 (2013) 66–75

Contents lists available at ScienceDirect

Biophysical Chemistry

journal homepage: http://www.elsevier.com/locate/biophyschem

Interaction of bee venom toxin melittin with ganglioside GM1 bicelle

Ummul Liha Khatun, Chaitali Mukhopadhyay *

Department of Chemistry, University of Calcutta, 92, A.P.C. Road, Kolkata 700009, India

HIGHLIGHTS

- Percentage of melittin bound to GM1 bicelles is higher than that of control PC bicelles.
- Percentage of melittin bound to GM1 bicelles is higher than that of GM1 micelles.
- Melittin is fully α-helical in the presence of control PC bicelles.
- In GM1 containing bicelles melittin becomes partially folded.
- Lytic activity of melittin is less in the presence of GM1 bicelles than that of PC bicelles.

GRAPHICAL ABSTRACT

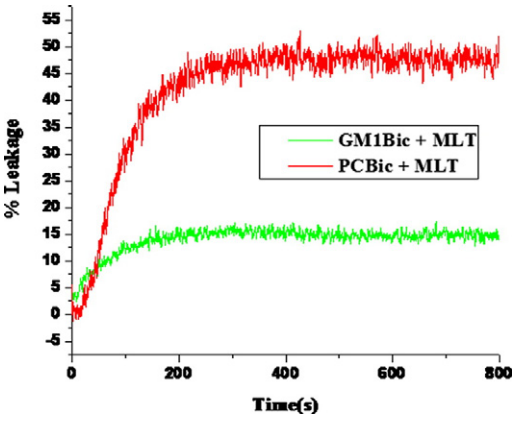

ARTICLE INFO

Article history:
Received 8 April 2013
Received in revised form 14 June 2013
Accepted 17 June 2013
Available online 22 June 2013

Keywords:
Melittin
GM1
Bicelle
Leakage
DOSY
CD

ABSTRACT

Melittin is a bee venom toxin that can act as antimicrobial peptide. Gangliosides are glycosphingolipids that help maintain membrane structure and organization as well as act as anchors for lectins, toxins, pathogens and antimicrobial peptides. Here we investigate interaction of melittin with fast tumbling isotropic control DMPC/CHAPS bicelles and ganglioside doped DMPC/CHAPS/GM1 bicelles. DOSY result shows that larger percentage of peptide binds to GM1 containing bicelles than that of the control PC bicelles. Bound peptide induces leakage of the bicelles entrapped carboxyfluorescein. Percentage of leakage is higher from control PC bicelles than that of the GM1 containing bicelles. In the presence of control PC bicelles melittin acquired fully α-helical structure. But in the presence of GM1 containing bicelles the peptide is not fully α-helical i.e., some random coil structure is present in this folded form. The present study shows that GM1 has an effect on membrane active antimicrobial peptide melittin.

Abbreviations: MLT, Melittin; GM1, Ganglioside Monosialo 1; DMPC, 1,2-dimyristoyl-sn-glycero-3-phosphatidylcholine; CHAPS, 3-[(3-Cholamidopropyl) dimethylammonio]-1-propanesulfonate; DHPC, 1,2-dihexanoyl-sn-glycero-3-phosphocholine; DMPG, 1,2-dimyristoyl-*sn*-glycero-3-[phospho-rac-(1-glycerol)]; NMR, Nuclear Magnetic Resonance; DOSY, Diffusion Ordered Spectroscopy; CD, Circular Dichroism; REES, Red Edge Excitation Shift; TCSPC, Time Correlated Single-Photon Counting; AMP, Anti Microbial Peptide; CF, Carboxyfluorescein.

* Corresponding author at: Department of Chemistry, University of Calcutta, 92, A.P.C. Road, Kolkata-700 009, India. Tel.: +91 033 2351 8386; fax: +91 033 2351 9755.
E-mail addresses: chaitalicu@yahoo.com, cmchem@caluniv.ac.in (C. Mukhopadhyay).

0301-4622/$ – see front matter © 2013 Elsevier B.V. All rights reserved.
http://dx.doi.org/10.1016/j.bpc.2013.06.012

1. Introduction

Melittin (MLT) is a naturally occurring cationic anti microbial peptide (AMP) obtained from the toxic component in the venom of the European honey bee, *Apis mellifera* [1]. It is a small linear peptide composed of 26 amino acids having the sequence NH2-GIGAVLKVLTTGLPALISWIKRKRQQ-CONH2 [2]. The amino-terminal region (residues 1–20) of this peptide is predominantly hydrophobic whereas the carboxy-terminal region (residues 21–26) is hydrophilic due to the presence of a stretch of positively charged amino acids [2]. Due to this amphiphilic property of MLT it becomes water-soluble and spontaneously associates with natural and artificial membranes [3]. Because of poor cell selectivity, it exhibits strong lytic activity against both bacterial and mammalian cells. At a moderately high concentration, MLT is known to cause micellization as well as membrane fusion, in addition to voltage-dependent ion channel formation across the planar lipid bilayer [4]. MLT is intrinsically fluorescent due to the presence of a single tryptophan residue at the 19th position. The presence of this tryptophan at the 19th position is utilized as the probe to study the interaction of MLT with membranes and membrane-mimetic systems [2–6]. The organization and dynamics of the tryptophan are important for the function of the MLT [7–9]. It is reported that uniquely positioned tryptophan is responsible for maintaining the structure and lytic activity of MLT [7–9].

Apart from its physiological functions, MLT has very interesting conformational properties also [10]. MLT adopts a predominantly random coil conformation and exists as monomer in aqueous solution at low pH, low concentration and low ionic strength [11]. At high ionic strength (i.e., in the presence of 2 M NaCl), at higher concentration (more than 4 mM) and at high pH MLT self-associates to form an α-helical tetrameric structure, driven by the formation of a hydrophobic core [11,12]. MLT adopts an α-helical conformation upon binding to lipid membranes or micelles [13,2]. NMR studies show that when MLT is bound to membrane it adopts α-helical conformation with a kink (at Pro14 residue) in the middle [14,15].

Interactions of MLT with natural as well as artificial membranes are extensively investigated in order to elucidate the mechanism of the physiological activity of the peptide [10,12,16-22]. By ultracentrifugation and quasi-elastic light-scattering measurements it is shown that melittin forms stoichiometrically well-defined complexes with dodecylphosphocholine micelles [23]. Evidence from circular dichroism indicates that the conformation of melittin bound to micelles of various detergents or of diheptanoyl phosphatidylcholine is largely independent of the type of lipid and furthermore appears to be quite closely related to the α-helical conformation as observed in phospholipid bilayer [23]. MLT interacts with negatively charged lipids with 100-fold greater affinity than with zwitterionic lipids [12,24]. This has been proven experimentally in a series of binding studies on MLT with phospholipids [24–27]. It was suggested that MLT tends to be adsorbed on the surface of the negatively charged membrane due to the electrostatic interaction, while it is adsorbed into the hydrophobic core of the membrane for the electrically neutral membrane [10]. The presence of negatively charged lipids in the membrane has been shown to inhibit membrane lysis by MLT and this inhibition is enhanced with increasing surface charge density [10,28–32].

Gangliosides, the most complex of glycosphingolipids, are abundant in the plasma membrane of nerve cells (making up 5–10% of the total lipid mass) and are found widely in most vertebrate cell types [33,34]. Gangliosides are acidic glycolipids showing strong amphiphilic character with the hydrophobic ceramide moiety inserted into the external leaflet of the cell membrane and the hydrophilic oligosaccharide head group with one or more *N*-acetyl neuraminic acids (sialic acid) faced toward the extracellular space [34]. Ganglioside takes part in cell-to-cell communication and in signal transduction [35–38]. Gangliosides are important component of lipid microdomains or raft that mediate protein sorting, transport and signal transduction [39]. Ganglioside is involved in a variety of biological process e.g., neurite outgrowth [40,41], cell division [42], regulation of receptor function etc [43]. The most well-known biological function of GM1 is to act as the cell surface receptor for the *Vibrio cholera* toxin and *Escherichia coli* heat-labile enterotoxin [44–46] as well as for viruses such as simian rotavirus [47a]. Recently, it has been reported that ganglioside serves as a molecular portal for the cellular interaction of AMP Magainin-2 [47b].

The rigorous search for a sensitive and innovative model membrane during the last 25 years has resulted in a new model called 'bicelles'. Bicelles are composed of aliphatic long (12–18 carbons) chain lipids and either short (6–8 carbons) chain lipids or detergent [47c]. Long chain lipids reside in planer disk region and form bilayer whereas short chain lipids or detergent resides at the rim [47c]. The properties of bicelles are strongly dependent on several physical parameters of which the key parameter of bicelles is the q-value. 'q' is defined as the molar ratio of long chain lipids to that of short chain lipids or detergent [47c]. The size and shape of bicelles are highly controlled by the q value [47c]. At smaller q value ($q < 1$), bicelles are known to have fast tumbling and isotropic properties in aqueous solution with discoidal shape.

Here we report an interaction of membrane active peptide MLT with ganglioside GM1-doped fast tumbling isotropic ternary bicelles ($q = 0.25$), composed of 1,2-dimyristoyl-sn-glycero-3-phosphocholine(DMPC), 3-(cholamidopropyl)-dimethylammonio-2-hydroxyl-1-propane-sulfonate(CHAPS) and GM1 (1:4:0.3 mol ratio), through fluorescence and DOSY approaches. We have used circular dichroism to monitor the structure of MLT in the presence of GM1 containing bicelle. We have also used the red edge excitation shift (REES) to monitor the organization and dynamics of tryptophan residues of MLT in the presence of bicelle. We have done leakage experiment to monitor the lytic activity of MLT. To the best of our knowledge this is the first study indicating that ganglioside containing model membrane may resist melittin's lytic property to some extent. We have very conclusively shown that there is more tendency of ganglioside containing membrane to interact with melittin than that of the control phospholipid membrane.

2. Material and methods

2.1. Materials

Melittin, DMPC (1,2-dimyristoyl-sn-glycero-3-phosphosphatidylcholine), and CHAPS [(3-cholamidopropyl)-dimethylammonio-2-hydroxyl-1-propane-sulfonate] were purchased from Sigma Aldrich Pvt. Ltd. (USA) and used without further purification. GM1 was isolated and purified from a goat brain in our laboratory following the published protocol [10]. Milli-Q water was used throughout the experiment to avoid salt interference on the binding of peptide to the negatively charge GM1 containing bicelles.

2.2. Bicelle preparation

Control phospholipid bicelles were prepared taking DMPC/CHAPS at 1:4 mol ratio and ganglioside containing bicelles i.e. DMPC/CHAPS/GM1 bicelles were prepared using DMPC/CHAPS/Ganglioside at 1:4:0.3 mol ratio following our published protocol [48,49]. Briefly, to prepare DMPC/CHAPS bicelles appropriate amount of DMPC was weighted first and then suspended in Milli-Q water of pH 5.5. Hydrated samples were centrifuged and then vigorously stirred in a vortex mixer followed by centrifugation at room temperature until homogenous slurry was formed. Now appropriate amount of CHAPS from 400 mM stock solution (in Milli-Q water of pH 5.5) was added to the slurry so that q becomes 0.25 and followed by vortex until a clear and transparent solution was obtained.

To prepare ganglioside GM1 doped bicelles appropriate amount of DMPC and ganglioside (GM1) was weighted. Now stocked ganglioside and DMPC were suspended in Milli-Q water of pH 5.5 to prepare homogeneous slurry. Appropriate amount of CHAPS from 400 mM stock solution (in Milli-Q water of pH 5.5) was added to the slurry to make the solution clear and transparent following the above stated protocol. Milli-Q water of pH 5.5 was used for bicelle preparation. The pH was adjusted by adding small volumes of 1 M HCl or 1 M NaOH. No buffer was used in order to keep the ionic strength minimum [48,49].

2.3. Steady-state fluorescence measurements

Steady state fluorescence measurements were performed with a Perkin-Elmer LS-55 spectrofluorometer at room temperature using 1 cm path length quartz cuvettes. Excitation and emission slits with a nominal band pass of 5 nm were used for all measurements. An excitation wavelength of 295 nm was used for all the experiments. Background intensities of Milli-Q water, PC bicelles and the GM1 containing bicelles without MLT were subtracted from each MLT containing spectrum to discard any contribution from the solvent. For steady state fluorescence bicelles concentration was 30 mM. Samples containing MLT were produced by adding an amount of powdered MLT corresponding to a concentration of 300 μM to the ready-made bicelle solution followed by vortexing so that peptide bicelle mol ratio becomes 1:100.

2.4. Fluorescence quenching measurements

For acrylamide quenching bicelle concentration was 30 mM and peptide bicelle mol ratio was 1:100. Acrylamide quenching experiments of 300 μM MLT fluorescence in two types of bicelles and in aqueous solution were carried out by measurement of the fluorescence intensity of MLT in water and two bicellar systems in separate samples by adding increasing concentrations of acrylamide taken from a freshly prepared stock solution (2 M) in water. Samples were incubated in the dark for 1 h before measuring the fluorescence. The fluorescence quenching experiments were performed using a Perkin-Elmer LS-55 spectrometer at room temperature. For acrylamide quenching measurements the excitation wavelength used was 295 nm and emission was monitored at the fluorescence emission maximum of melittin in water and in given bicellar system.

Quenching data were analyzed by fitting them to the classical Stern–Volmer equation

$$F_0/F = 1 + K_{SV}[Q] = 1 + k_q \iota_0 [Q] \quad (1)$$

where F_0 and F are the fluorescence intensities in the absence and presence of the quencher respectively, [Q] is the molar quencher concentration and K_{SV} is the Stern–Volmer quenching constant. The Stern–Volmer quenching constant K_{SV} is equal to $k_q \iota_0$ where k_q is the bimolecular quenching constant and ι_0 is the lifetime of the fluorophore in the absence of quencher.

2.5. Time-resolved fluorescence measurements

Fluorescence lifetimes were obtained by the method of Time Correlated Single-Photon Counting (TCSPC) on FluoroCube-01-NL spectrometer (Horiba Jobin Yvon) using a nanoLED as light source (290 nm) and the signals were collected at the magic angle of 54.7° to eliminate any considerable contribution from fluorescence anisotropy decay. For TCSPC same concentration of bicelle, peptide and bicelle peptide mole ratio was used as that of steady state fluorescence. The decays were deconvoluted using DAS-6 decay analysis software. The acceptability of the fits was judged by χ^2 criteria (fitting analysis having $1.20 < \chi^2 < 1.00$ has been negated) and visual inspection of the residuals of the fitted function to the data. The mean lifetimes for the decay curves were calculated from the decay times and the relative contribution of the components using the following relation,

$$\langle \tau_0 \rangle = \frac{\sum_i \alpha_i {\tau_i}^2}{\sum_i \alpha_i \tau_i} \quad (2)$$

where $<\tau_0>$ is the mean lifetime of tryptophan.

2.6. Melittin-induced leakage experiments

The leakage induced by melittin was measured at room temperature by recording the release of bicelle-encapsulated carboxyfluorescein. For leakage experiments bicelle concentration was 30 mM and MLT concentration was 300 μM so that peptide bicelle mol ratio remains 1:100. Bicelles loaded with carboxyfluorescein were prepared as follows.

For control PC bicelles appropriate amount of DMPC and dye [carboxyfluorescein, corresponding to a weight of 50 mM concentration] was weighted. Stock DMPC and dye was dissolved in chloroform: methanol 2:1 solution. Samples were vortexed and then dried under a stream of nitrogen gas. Residual solvent was removed by placing the samples under high vacuum overnight. After this procedure, appropriate amount of CHAPS from 400 mM stock solution (in milliQ H_2O of pH 5.5) was added to the dried lipid film so that q becomes 0.25 followed by vortexing until the sample becomes transparent. Finally carboxyfluorescein loaded bicelle solution was dialyzed against milliQ H_2O of pH 5.5 to remove excess untrapped dye. For GM1 containing bicelles appropriate amount of DMPC, GM1 and carboxyfluorescein was weighted. Stock solution of DMPC, GM1 and carboxyfluorescein was dissolved in chloroform:methanol 2:1 solution. The rest of the steps were performed using same protocol as that of control PC bicelles.

Fluorescence was measured at room temperature (25 °C) with a Perkin-Elmer LS-55 spectrofluorometer using 1 cm path length quartz cuvettes. The excitation wavelength was 492 nm and emission was set at 517 nm. Excitation and emission slits with a nominal band-pass of 5 nm were used. The encapsulated carboxyfluorescein resulted in low background fluorescence intensity of the bicelle solution (I_B). Melittin was added to the bicelle solution leading to the release of carboxyfluorescein into the medium. This leakage of the dye was monitored by measuring the increase in fluorescence intensity. After a rapid release of the probe, occurring over a period of about 200 s, the fluorescence intensity remains almost constant; the fluorescence intensity used to calculate the release (I_F) was measured when the plateau was reached. The experiments were normalized relative to the total fluorescence intensity (I_T), measured after complete disruption of all the bicelles by Triton X-100 (0.1 vol.%). CF release could not be detected with bicelles alone (without any addition of melittin) in the time scale of the experiment. The percentage of released carboxyfluorescein was calculated according to the following equation:

$$\% \text{ release} = 100(I_F - I_B)/(I_T - I_B).$$

2.7. CD measurements

Far UV-CD spectra were acquired on a MOS-450 spectrometer using a silica quartz cell of 0.1 cm path length at room temperature. Records were averaged over 3 scans collected over the interval of 190 to 250 nm. Background spectra of Milli-Q water (pH 5.5), DMPC/CHAPS bicelles and DMPC/CHAPS/GM1 bicelles were used as control and were subtracted from each of the peptide containing spectra in water and in the presence of bicelles. The respective intensities are expressed in terms of mean residue molar ellipticity $[\theta] = 100[\theta]_{obs} / CLn$, where $[\theta_{obs}]$ is the observed ellipticity in millidegrees, L is the optical path length in centimeter (0.1 cm in the present case), n is the number of amino acid

residues and C is the molar concentration of the peptide. For circular dichroism spectroscopy bicelle concentration was 30 mM and MLT concentration was 300 μM so that peptide bicelle mol ratio becomes 1:100.

2.8. Collection and processing of diffusion NMR data

As NMR is of low sensitivity compared to fluorescence or CD so for DOSY experiment concentration of bicelles used was 90 mM and peptide concentration was 900 μM to maintain peptide bicelle mol ratio 1:100. Diffusion-ordered spectroscopy (DOSY) experiments were performed on the Bruker Avance 600 MHz spectrometer. The pulse sequence used a stimulated echo with bipolar gradient pulses and two spoil gradient followed by a 3-9-19 pulse for water suppression. The gradient strength was increased from ~2% to 95% of the maximum gradient strength in 32 increments to attenuate the ^{1}H signal ~5% to their initial amplitude. The diffusion time Δ was 150 ms and the gradient duration δ was 5 ms. The DOSY spectra were processed using DOSYToolbox (v 0.53) [50]. Diffusion coefficient (D) was calculated by fitting the curve of signal intensity versus variable gradient strength via use of SCORE component analysis. Exclude region command was used to correct the noise and inconsistencies in the spectra which may affect a particular signal intensity. Gaussian line shape with a single exponential fit was applied to optimize the resolution of signals. The individual diffusion coefficients were calculated from DOSY using aliphatic Leu/Ile-Hδ1/Hδ2 peak resonates at about 0.89 ppm for the peptide. For DMPC and CHAPS the individual diffusion coefficients were calculated from the DOSY spectra using selective aliphatic acyl chain methylene (at 1.20 ppm, Fig. 8) for DMPC and methyl region protons of CHAPS (position 19 at 0.8 ppm and position 18 at 0.6 ppm, Fig. 8). The average bicellar diffusion coefficient was obtained by selecting specifically the non overlapping [51] aliphatic acyl chain methylene of DMPC plus terminal methyl region protons of CHAPS. The measured diffusion coefficient (Dobs) is given by the following equation [52].

$$D_{obs} = S_{bound} \cdot D_{bound} + S_{free} \cdot D_{free}$$

$$D_{obs} = S_{bound} \cdot D_{bound} + (1 - S_{bound}) \cdot D_{free}$$

where S_{free} and S_{bound} are the mole fractions of free and bound peptides respectively. D_{free} is obtained by measuring the diffusion coefficient of peptide in water and D_{bound} corresponds to the diffusion coefficient of the bicelles. In bicellar environment, diffusion of the free peptide becomes slow due to the presence of bicelles themselves. Therefore, it is essential to correct D_{free} by introducing an obstruction factor such as:

$$D^{\phi}_{free} = D_{free}\langle A \rangle$$

where ϕ is the volume fraction of the obstructing particles and <A> is a correction factor for spherical objects. This factor has been calculated by Gaemers and Bax for a 10% w/w bicelle solution at 20 °C assuming spherical shape of the bicelle and gave <A> = 0.95 [53]. Our bicelle can be approximated as spherical objects, thus <A> = 0.95 can be used to calculate D^{ϕ}_{free} [52].

3. Results

3.1. Steady-State Fluorescence spectroscopy

We measured the intrinsic fluorescence of melittin in water, in the presence of PC bicelles and in the presence of GM1 containing bicelles and the results of steady state fluorescence are depicted in Fig. 1. In water, melittin shows the peak of tryptophan at 365 nm. In going from water to PC bicelles fluorescence intensity increases and also undergoes a blue shift of 21 nm. In going from water to GM1 containing bicelles a blue shift of 19 nm was observed. In other words in going from PC bicelles to GM1 containing bicelles red shift occurs with a decrease in fluorescence intensity.

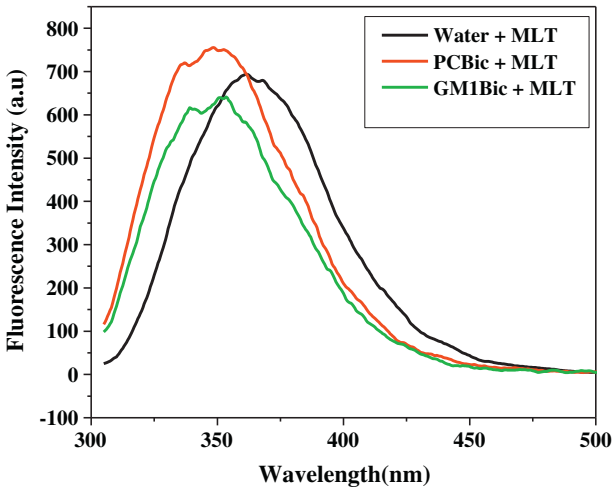

Fig. 1. Intrinsic tryptophan fluorescence spectra for melittin at 25 °C in water, DMPC/CHAPS (1:4) bicelles and DMPC/CHAPS/GM1 (1:4:0.3) bicelles. Bicelle concentration was 30 mM and the peptide concentration was in all cases 300 μM (peptide: bicelle = 1:100 mol/mol). Individual plots are labeled in the figure.

3.2. Quenching of Trp fluorescence with acrylamide

Stern-Volmer plots for the quenching of tryptophan by acrylamide, recorded in the absence and presence of bicelle, are depicted in Fig. 2. Fluorescence intensity of tryptophan decreased in a concentration-dependent manner by the addition of acrylamide to the peptide solution both in the absence and presence of bicelles, without other effects on the spectra. For the acrylamide quenching the Stern–Volmer plots for monomeric melittin in water, in PC bicelles and in GM1 containing bicelles are linear indicating a dynamic quenching process. The Stern–Volmer constants (K_{SV}) of melittin in water, in PC bicelles and in GM1 containing bicelles are 19.03, 2.37 and 5.25 M^{-1} respectively.

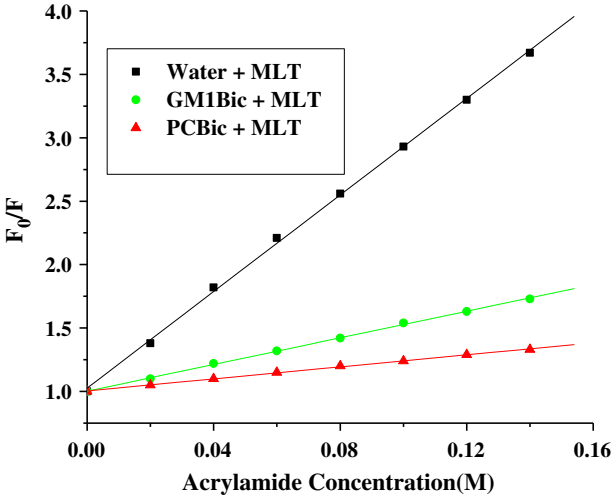

Fig. 2. Representative data for Stern–Volmer analysis of acrylamide quenching of melittin in water, PC bicelles and GM1 containing bicelles. F_0 is the fluorescence in the absence of quencher, and F is the corrected fluorescence in the presence of quencher. The excitation wavelength was 295 nm and emission was monitored as in Fig. 1. Bicelle concentration was 30 mM and the peptide concentration was in all cases 300 μM (peptide:bicelle = 1:100 mol/mol). Individual plots are labeled in the figure.

3.3. REES of melittin in presence of bicelles

The shifts in the maximum of the fluorescence emission of the tryptophan residue of melittin when bound to PC bicelles and GM1 containing bicelles as a function of excitation wavelength are shown in Fig. 3. As the excitation wavelength is changed from 280 to 305 nm, the emission maxima of bicelle-bound melittin are shifted from 346 to 349 nm in case of GM1 containing bicelles, and from 344 to 351 nm for PC bicelles which correspond to a REES of 3 and 7 nm respectively. Such dependence of the emission spectra on the excitation wavelength is characteristic of the red-edge effect.

3.4. Time-resolved fluorescence

The fluorescence lifetime serves as a faithful indicator of the local environment in which a given fluorophore is placed [2]. A typical decay profile of the tryptophan residue of melittin in water, PC bicelles and GM1 containing bicelles with its biexponential fitting is shown in Fig. 4. The fluorescence lifetimes of melittin in water, PC bicelles and GM1 containing bicelles are shown in Table 1. In general, a decrease in polarity of the tryptophan environment increases the lifetime of the excited state of tryptophan due to slow deactivation processes in nonpolar environment. Although the mean fluorescence lifetime of the excited state of tryptophan residue of melittin in the three media i.e., water, PC bicelles and GM1 containing bicelles differ very slightly but the components of lifetime [fast and slow] in the three media differ significantly. Components of lifetime of the tryptophan residue of melittin in water was found to be 1.648 ns and 3.68 ns. PC bicelles have two components with lifetime 1.440 ns and 4.624 ns while that for GM1 containing bicelles these are 1.403 ns and 4.516 ns.

3.5. Melittin-induced leakage of bicelle contents

The membrane permeabilizing activity of melittin was evaluated by conducting CF leakage experiment. Fig. 5 shows the % of release of CF, entrapped in DMPC/CHAPS (1:4) bicelles and DMPC/CHAPS/GM1 (1:4:0.3) bicelles, induced by melittin. As is evident from the figure, the lytic efficiency of melittin in different bicelles is clearly dependent on the composition of the membrane. Thus, while there is about 45% lysis in DMPC/CHAPS (1:4) bicelles, it is reduced to 12-15% for DMPC/CHAPS/GM1 (1:4:0.3) bicelles at the same bicelle/peptide ratio.

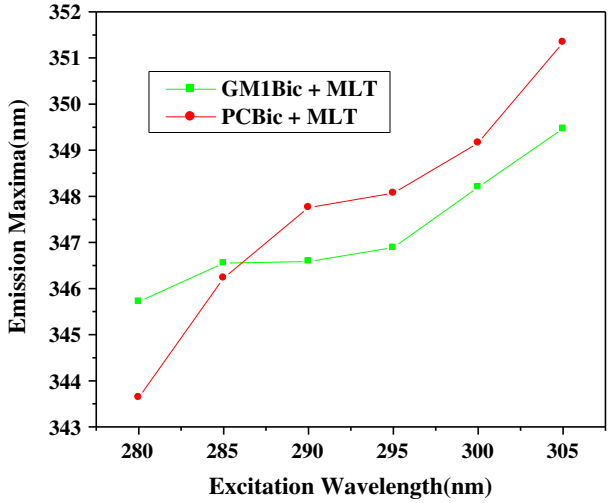

Fig. 3. Effect of changing the excitation wavelength on the wavelength of the maximum emission of melittin in DMPC/CHAPS (1:4) bicelles,and DMPC/CHAPS/GM1 (1:4:0.3) bicelles. Bicelle concentration was 30 mM and the peptide concentration was in all cases 300 μM (peptide:bicelle = 1:100 mol/mol). Individual plots are labeled in the figure.

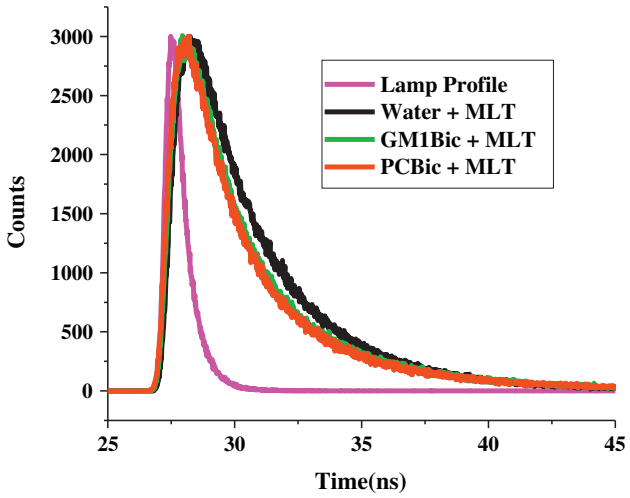

Fig. 4. Time-resolved fluorescence intensity decay of melittin in water, PC bicelles and GM1 containing bicelles. The excitation wavelength was at 290 nm, which corresponds to a peak in the spectral output of the nitrogen lamp. Emission was monitored at 365,344 and 346 nm for melittin in water, PC bicelle and GM1 bicelle respectively. The sharp peak on the left is the lamp profile. The relatively broad peaks on the right are the decay profiles, fitted to a biexponential function. Individual plots are labeled in the figure.

3.6. Circular dichroism spectroscopy

CD spectra were recorded for melittin in water, control DMPC/CHAPS (1:4) bicelles and DMPC/CHAPS/GM1 (1:4:0.3) bicelles and the results are represented in Fig. 6. CD spectroscopy of melittin in water shows minima around 202 nm indicating that the peptide adopts random coil structure in water. In the presence of DMPC/CHAPS bicelles melittin adopts completely α-helical structure evident from the two characteristic minima at 208 nm and 222 nm. In GM1 containing bicelles minima observed around 210 nm indicates that in the presence of GM1 containing bicelles the peptide is not fully α-helical i.e., some random coil structure is present in this folded form.

3.7. Analysis of translational diffusion measurements

Translational diffusion measurements are summarized in Table 2 and the DOSY spectra of MLT in the presence of GM1 containing bicelles is depicted in Fig. 7. Diffusion coefficient of melittin in water is 18.6×10^{-11} m^2/s which decreases in either of the bicelles. In the presence of PC bicelles diffusion coefficient of melittin is 15.5×10^{-11} m^2/s and in the presence of GM1 containing bicelles diffusion coefficient of melittin is 13.4×10^{-11} m^2/s. From diffusion NMR it has been observed that 44% melittin is bound to GM1 containing bicelles where as 29% melittin bound to PC bicelles.

4. Discussion

Influence of ganglioside GM1 on bee venom toxin melittin has been previously investigated from our lab by interacting melittin with GM1 micelle [10,54]. Here we investigate the effect of ganglioside GM1 on

Table 1
Fluorescence lifetimes and fitting parameters of melittin in water, PC bicelles and GM1 containing bicelles obtained by biexponential fitting.

Medium	α1	τ1(ns)	α2	τ2(ns)	Mean τ
Water	0.43	1.648	0.57	3.681	3.168
PC Bic	0.74	1.440	0.26	4.624	3.128
GM1 Bic	0.73	1.403	0.27	4.516	3.095

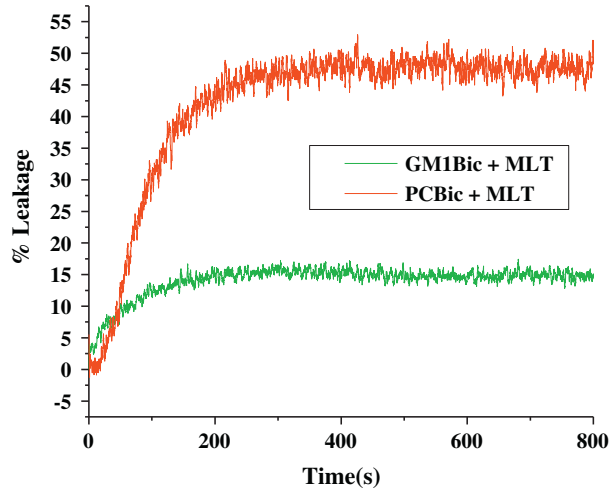

Fig. 5. Membrane permeabilizing activity of melittin. Percent leakage values of carboxyfluorescein entrapped within bicelles plotted as a function of Times. The total lipid concentration was 30 mM and the peptide concentration was in all cases 300 μM (peptide:bicelle = 1:100 mol/mol). Individual plots are labeled in the figure.

melittin by interacting melittin with DMPC/CHAPS/GM1 (1:4:0.3) bicelles. Although membrane mimicking property of micelle has long been used to study the structure and dynamics of membrane active peptides, now-a-days bicelles have emerged as more popular membrane models. This is because of the fact that small size i.e, large curvature of micelles influences peptide conformation and dynamics more where bicelles are reportedly capable of providing more biologically relevant diversified conformations and dynamics of proteins/peptides. In addition, bicelles have higher morphological similarity with native bilayers [55]. Superiority of bicelle can be justified from some recent reports. In DMPC/DHPC bicelles, a bilayer is formed which successfully solubilized the intact outer membrane protein OmpX from *E. coli* [56]. In another report Kang et al. have shown that DMPG/DHPC bicelles can deliver a functional membrane protein KCNE3 to oocyte membrane that expresses human KCNQ1 channels [57]. In our laboratory we have prepared ternary bicelles composed of DMPC, CHAPS and ganglioside GM1 and this ganglioside containing bicelles imparts biologically active receptor recognized conformation to leucine enkephalin, substance P

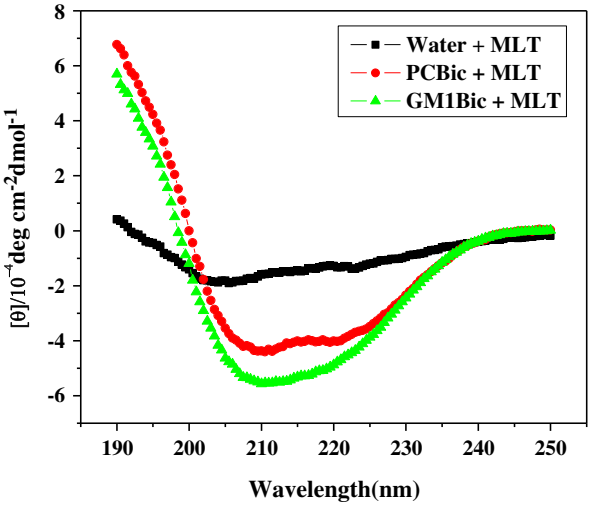

Fig. 6. Far-UV CD spectra of melittin in water, DMPC/CHAPS (1:4) bicelles and DMPC/CHAPS/GM1 (1:4:0.3) bicelles at pH 5.5 and 298 K. Bicelle concentration was 30 mM and peptide concentration was in all cases 300 μM (peptide:bicelle = 1:100 mol/mol). Individual plots are labeled in the figure.

Table 2
Measured translational diffusion coefficients of melittin and bicellar components DMPC and CHAPS in solution using DOSY and calculated fraction (%) of peptide bound to bicelles (pH 5.5 and 298 K).

Samples	$D_{obs} \pm 0.1(\times 10^{-11}$ m^2/s)				
	MLT	DMPC	CHAPS	Bicelle	%bound
MLT/water	18.6				
DMPC: CHAPS bicelle		10.5	11.4	9.5	
MLT/DMPC: CHAPS bicelle	15.2	9.3	11.7	9.1	29
DMPC: CHAPS: GM1 bicelle		8.9	11	8.6	
MLT/DMPC: CHAPS:GM1 bicelle	13.4	8.4	11	8.0	44

and neurotensin [49,48,58]. A very recent report has shown that unstructured N-terminal segment (1-30) of α-synuclein exhibited chemical shift changes upon interaction with the GM1 bicelles, but the conformation was less ordered compared to α-helical conformation previously reported in ganglioside micelles or ganglioside-embedded vesicles [59] and this is also supported by our observation on substance P.

We measured the intrinsic tryptophan fluorescence (Fig. 1) of melittin in water, in the presence of control PC bicelles and in the presence of GM1 containing bicelles to evaluate the degree of penetration of the peptides into the membrane bilayer. In going from water to bicelles blue spectral shift occurs which implies that in the presence of bicelles the tryptophan residue of the protein moves to a more hydrophobic environment. Blue spectral shift is larger in case of PC bicelles than that of GM1 containing bicelles i.e., in going from PC bicelles to GM1 containing bicelles red spectral shift occurs with a decrease in fluorescence intensity. This result indicates that melittin interacts with both control PC bicelles and GM1 containing bicelles but the tryptophan residue of melittin undergoes deeper insertion in the hydrophobic core of the membrane in PC bicelles than that of GM1 containing bicelles.

We have studied the accessibility of the tryptophan residue of membrane bound peptide towards acrylamide (Fig. 2), a water-soluble highly efficient quenching molecule, which is unable to penetrate into the hydrophobic core of the lipid bilayer. The more deeply a tryptophan residue is buried, the less strongly it can be quenched by acrylamide. High value of quenching constant indicates that in water the tryptophan residue is completely exposed. The large reduction of quenching constant in the presence of bicelles towards collisional quencher acrylamide clearly indicates considerable shielding of the tryptophan residue from its aqueous environment. It is interesting to note that K_{SV}'s are lowest for melittin in PC bicelles than that of GM1 containing bicelles indicating that in the presence of PC bicelles tryptophan residue of melittin is maximally shielded.

REES represents a powerful approach to directly monitor the environment and dynamics around a fluorophore in an organized molecular assembly [2]. A shift in the wavelength of the maximum fluorescence emission toward higher wavelengths, caused by a shift in the excitation wavelength toward the red edge of the absorption band, is termed REES [2]. This effect is mostly observed with polar fluorophores in motionally restricted media such as viscous solutions or condensed phases, where the dipolar relaxation time for the solvent shell around a fluorophore is comparable to or longer than its fluorescence lifetime [2]. REES therefore arises from slow rates of solvent relaxation (reorientation) around an excited state fluorophore, which is a function of the motional restriction imposed on the solvent molecules in the immediate vicinity of the fluorophore [2]. Utilizing this approach, it becomes possible to probe the mobility parameters of the environment itself (which is represented by the relaxing solvent molecules) using the fluorophore merely as a reporter group [2]. Observation of this effect in bicelles implies that melittin, when incorporated in bicelles, is in an environment where its mobility is considerably reduced, such a result would directly imply

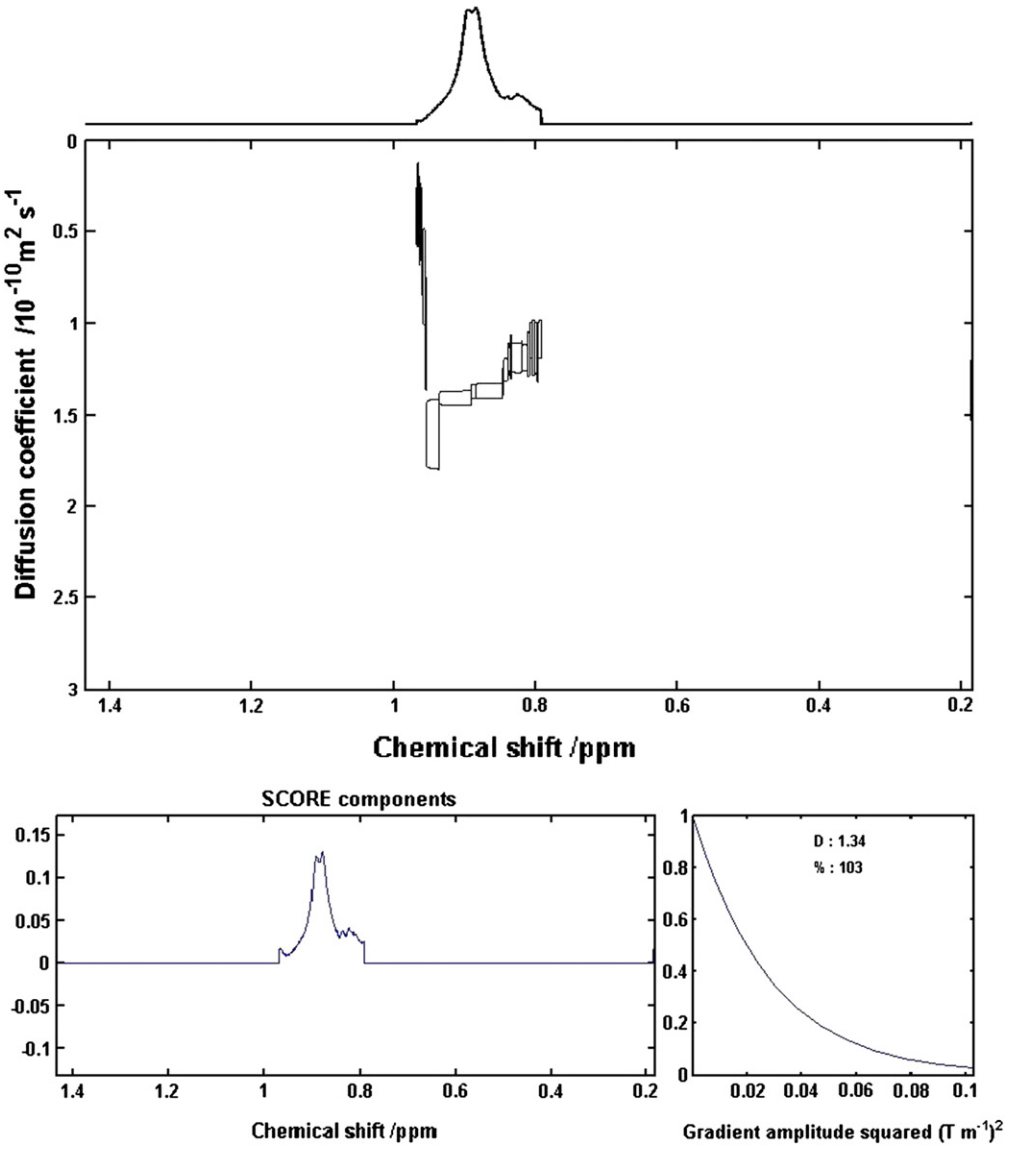

Fig. 7. Selective leucine/isoleucine $H_{\delta 1}/H_{\delta 2}$ region in DOSY (top) and plot of ln (I/I_0) vs G^2 (bottom) of melittin in the presence of GM1 containing bicelles at pH 5.5 and 298 K.

that this region of the bicelles offer considerable restriction to the reorientational motion of the solvent dipoles around the excited state fluorophore. As the excitation wavelength is changed from 280 to 305 nm, the emission maximum of melittin in water remains invariant at 365 nm, irrespective of the excitation wavelength. Melittin therefore does not exhibit REES in water. The magnitude of REES (Fig. 3) is less for melittin in GM1 containing bicelles compared to REES obtained in control PC bicelles, indicating that tryptophan residue of melittin resides in a less restricted environment in the presence of GM1containing bicelles where as the tryptophan residue is in more restricted environment in the presence of control PC bicelles.

From TCSPC (Fig. 4 and Table 1) it has been observed that in going from water to bicelles although the contribution of the component with shorter lifetime differs slightly but the contribution of the component with the longer lifetime increases significantly. This result indicates that in going from water to bicelles tryptophan residue of melittin moves in a less polar environment, decreased water penetration in the interfacial region of membranes. Lifetime of the components differs slightly between GM1 containing bicelles and PC bicelles indicating that the local environment experienced by the tryptophan residue is slightly different in two cases i.e, tryptophan residue is slightly more restricted in PC bicelles than that of the GM1 containing bicelles.

Though translational diffusion coefficient measurement for GM1 at the present concentration is impossible here, but its impact is clear from translational diffusion measurement. Translational diffusion coefficients indicate that the incorporation of GM1 in DMPC/CHAPS bicelles hinders the diffusion of DMPC because phospholipid mobility gets restricted (Table 2). On the other hand no change in CHAPS diffusion coefficient also suggests that GM1 is localized along with the long chain PC molecules (Table 2). Gangliosides are large molecules having two hydrocarbon chains along with a large oligosaccharide headgroups and reside mostly in the exoplasmic leaflet of the cell membrane in proximity towards the extracellular space fluid. Diffusion coefficient of melittin in water is 18.6×10^{-11} m^2/s which is reduced in either of the bicelles (Table 2). The decrease in the diffusion coefficient of the peptides in the presence of bicelles is clearly indicating the interaction of peptide with the bicelles. Diffusion of the peptide is slower in the presence of GM1 containing bicelles than the PC bicelles (Table 2) which implies that peptide interaction is stronger with GM1 containing bicelles than that of the control PC bicelles. Thus, translational diffusion results indirectly show the effect of ganglioside GM1 on MLT. Translational diffusion coefficient of CHAPS is comparatively larger than diffusion coefficient of DMPC and this is due to the fact that size of CHAPS is smaller than DMPC. Interaction of the peptide to the bicelles decreases

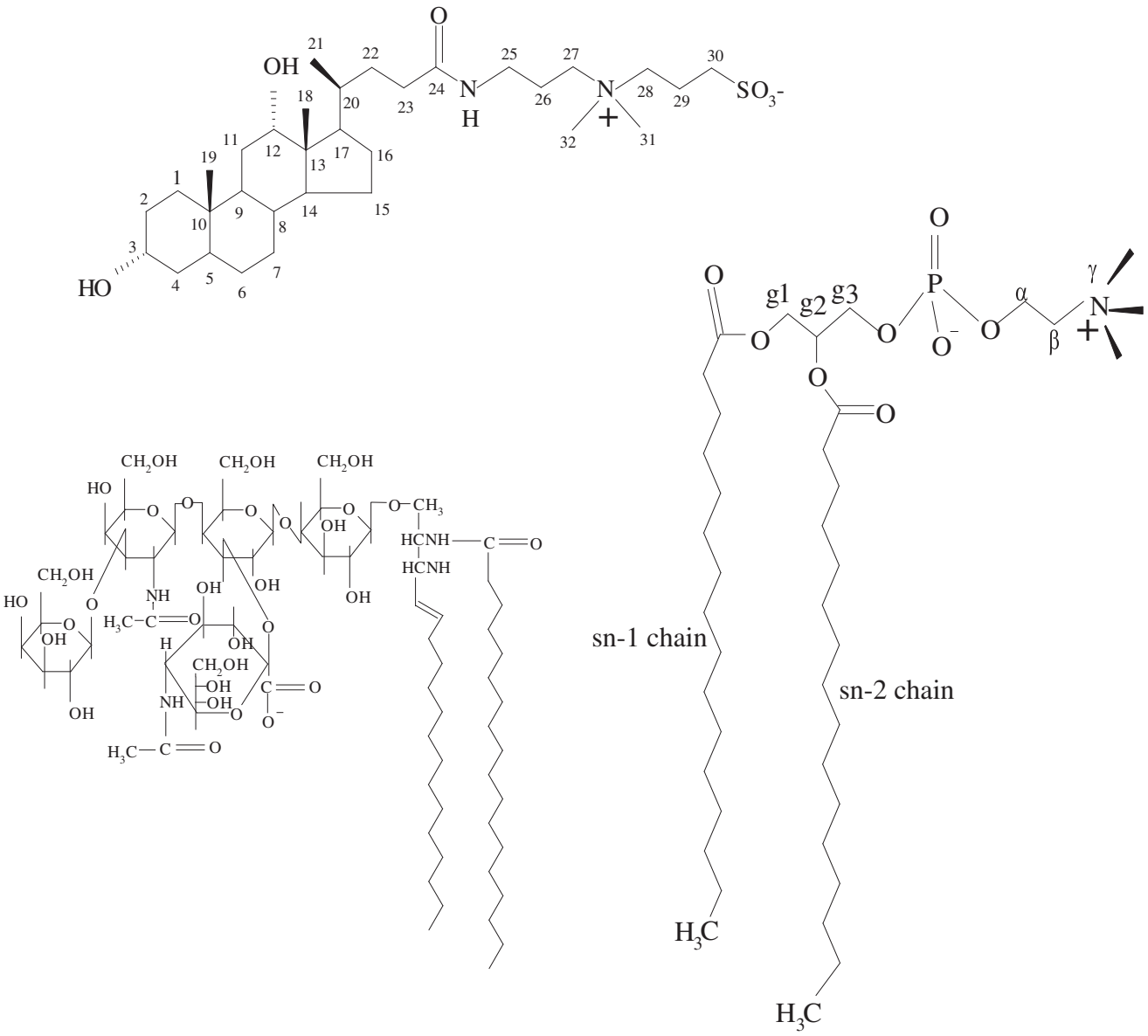

Fig. 8. Structure of DMPC (lower right panel), CHAPS (upper left panel) and GM1 (lower left panel).

the diffusion coefficient of only DMPC whereas the presence of peptide does not alter the diffusion coefficient of CHAPS (Table 2). This result indicates that peptide prefers to reside at the bicellar low-curvature region and interact with long chain lipids. Percentage of MLT bound to GM1 containing bicelles is (44%) larger than that of the control PC bicelles (29%) (Table 2).

CD experiment (Fig. 6) provides the idea about the secondary structure of the peptide induced by its surrounding environments. In the presence of DMPC/CHAPS bicelles two characteristic minima at 208 nm and 222 nm were observed indicating a fully α-helical structure. In GM1 containing bicelles minima around 210 nm are observed indicating that in the presence of GM1 containing bicelles the peptide is not fully α-helical i.e., some random coil structure is present within folded form. The difference in binding affinity may be related to a difference in the conformation of membrane-bound peptide. Previous study [54] from our lab has shown that in the presence of GM1 micelles MLT exist as fully α-helix. DOSY result shows that 32% MLT bounds to GM1 micelles [54] which are less than the percentage (44%) of MLT bound to GM1 bicelles. This difference in observation indicates that GM1 containing bicelles induces differences in membrane positioning and molecular dynamics of the peptide compared to GM1 micelles.

After the addition of melittin to bicelles there is an initial burst of leakage of carboxyfluorescein followed by a phase during which leakage slows down substantially consistent with the investigation of Wiedman et al. [60]. The burst phase occurs on a time scale of a few seconds (Fig. 5) which is similar to the time of peptide partition into bilayers [60]. As the percentage of binding of AMP melittin in GM1 containing bicelles is larger than that of the control PC bicelles so it may be expected that membrane permeabilization by MLT should be stronger towards GM1 containing bicelles than that of the PC bicelles. But in reality it has been observed that in GM1 containing bicelles membrane permeabilization is less than PC bicelles (Fig. 5). We have already shown specific interaction of GM1 with melittin using STD NMR [54]. From our another recent investigation [61] it has been observed by AFM and molecular modeling that head group of ganglioside GM1 protrudes out (1 nm) of the phospholipid head group. GM1 (ganglioside-monosialated) {Gal β (1-3) GalNac β (1-4) [NeuNac5Ac α (2-3)] Gal β (1-4) Glc β1-Cer} contains a pentasaccharide head group, of which four neutral sugars and one sialic acid. Sialic acid residue is negatively charged. So it may be expected

that positive charge containing melittin will be attracted by electrostatic interaction with the negative charge containing sialic acid of ganglioside and it is expected that melittin will remain closer to the head group region of gangliosides leading to weaker permeabilization. This is also supported from the fluorescence experimental studies indicating less non-polar environment of tryptophan in GM1 containing bicelles. It is also seen from the CD spectroscopy that in GM1 containing bicelles the acquired helicity of MLT is less than that in control PC bicelles. Together the facts indicate that though in GM1 bicelle, MLT is binding better, its lytic activity is less. This can be for several reasons: it might be due to inherent rigidity of GM1 containing membranes because of which the peptide is less incorporated, and it has less helicity. Thus the observed difference between GM1 containing bicelles and control phospholipid bicelles arising from ganglioside head group i.e., the observed differences is due to a specific interaction of MLT with GM1. This result is consistent with the observation of Miyazaki et al. [47b]. Recently Miyazaki et al. have reported that antimicrobial peptide Magainin 2 binds to the sugar region of GM1 consequently pore formation by Magainin 2 becomes much less effective in GM1/PC bilayer [47b].

5. Conclusion

Sting accident by honeybee causes severe pain, inflammation and allergic reaction. In addition to this hypersensitivity, an anaphylactoid reaction occurs by toxic effects even in a non-allergic person via cytolysis. Our result shows that in model nerve cell membrane or raft-like membrane where ganglioside is present lytic activity of melittin is less. In other words our study shows a potential of gangliosides to inhibit the disruptive effect of melittin and therefore may be used as therapeutic tools for melittin induced disruption of membrane. We have recently shown [61] that GM1 incorporates rigidity in the bicelle. Here we confirm the use of GM1-doped bicelle as not only a brain-membrane mimic that can induce biologically relevant conformation in the randomly structured melittin, but also a suitable delivery system. This was further shown from the melittin induce slower lysis.

Acknowledgments

This work acknowledges financial support of CSIR grant CSIR-01 (2400)/10/EMR-II and Nano project grant under sanction number CONV/002/NanoRAC/2008. We thankfully acknowledge the Central Facility of Saha Institute of Nuclear Physics, Kolkata for CD spectroscopy, and the Indian Association for Cultivation of Science for the NMR experiments. U.L.K. is thankful for CSIR fellowship under award no. 09/028(0701)/2008-EMR-I.

References

[1] E. Habermann, Bee and wasp venoms, Science 177 (1972) 314–322.
[2] H. Raghuraman, A. Chattopadhyay, Effect of micellar charge on the conformation and dynamics of melittin, European Biophysics Journal 33 (2004) 611–622.
[3] H. Raghuraman, A. Chattopadhyay, Influence of lipid chain unsaturation on membrane-bound melittin: a fluorescence approach, Biochimica et Biophysica Acta 1665 (2004) 29–39.
[4] M. Manna, C. Mukhopadhyay, Cause and effect of melittin-induced pore formation: a computational approach, Langmuir 25 (2009) 12235–12242.
[5] T.D. Bradrick, A. Philippetis, S. Georghiou, Stopped-flow fluorometric study of the interaction of melittin with phospholipid bilayers: importance of the physical state of the bilayer and the acyl chain length, Biophysical Journal 69 (1995) 1999–2010.
[6] H. Raghuraman, A. Chattopadhyay, Organization and dynamics of melittin in environments of graded hydration: a fluorescence approach, Langmuir 19 (2003) 10332–10341.
[7] S.E. Blondelle, R.A. Houghten, Hemolytic and antimicrobial activities of twenty-four individual omission analogues of melittin, Biochemistry 30 (1991) 4671–4678.
[8] E. Habermann, H. Kowallek, Modifications of amino group and tryptophan in melittin as an aid to recognition of structure–activity relationships, Hoppe-Seyler's Zeitschrift für Physiologische Chemie 351 (1970) 884–890.
[9] S.E. Blondelle, R.A. Houghten, Probing the relationships between the structure and hemolytic activity of melittin with a complete set of leucine substitution analogs, Peptide Research 4 (1991) 12–18.
[10] C. Chatterjee, C. Mukhopadhyay, Melittin–GM1 interaction: a model for a side-by-side complex, Biochemical and Biophysical Research Communications 292 (2002) 579–585.
[11] J. Bello, H.R. Bello, E. Granados, Conformation and aggregation of melittin: dependence of pH and concentration, Biochemistry 21 (1982) 461–465.
[12] C.E. Dempsey, The actions of melittin on membranes, Biochimica et Biophysica Acta 1031 (1990) 143–161.
[13] H.H. De Jongh, E. Goormaghtigh, J.A. Killian, Analysis of circular dichroism spectra of oriented protein–lipid complexes: toward a general application, Biochemistry 33 (1994) 14521–14528.
[14] A. Naito, T. Nagao, K. Norisada, T. Mizuno, S. Tuzi, H. Saito, Conformation and dynamics of melittin bound to magnetically oriented lipid bilayers by solid-state ^{31}P and ^{13}C NMR spectroscopy, Biophysical Journal 78 (2000) 2405–2417.
[15] Y.-H. Lam, S.R. Wassall, C.J. Morton, R. Smith, F. Separovic, Solid-state NMR structure determination of melittin in a lipid environment, Biophysical Journal 81 (2001) 2752–2761.
[16] F. Inagaki, I. Shimada, K. Kawaguchi, M. Hirano, I. Terasawa, T. Ikura, N. Go, Structure of melittin bound to predeuterated dodecylphosphocholine micelles as studied by two dimensional NMR and distance geometry calculations, Biochemistry 28 (1989) 5985–5991.
[17] A. Okada, K. Wakamatsu, T. Miyazawa, T. Higashijima, Vesicle bound conformation of melittin: transferred nuclear Overhauser experiment analysis in presence of perdeuterated phosphatidylcholine vesicles, Biochemistry 33 (1994) 9438–9446.
[18] P. Yuan, P.J. Fisher, F.G. Prendergast, M.D. Kemple, Structure and dynamics of melittin in lysomyristoyl phosphatidylcholine micelles determined by nuclear magnetic resonance, Biophysical Journal 70 (1996) 2223–2238.
[19] K. Hristova, C.E. Dempsey, S.H. White, Structure, location and lipid perturbations of melittin at the membrane interface, Biophysical Journal 80 (2001) 801–811.
[20] H. Vogel, F. Jahnig, The structure of melittin in membranes, Biophysical Journal 50 (1986) 573–582.
[21] C. Altenbach, W.L. Hubbell, The aggregation state of spin labeled melittin in solution and bound to phospholipid membranes: evidence that membrane-bound melittin in monomeric, Proteins 3 (1988) 230–242.
[22] J.C. Talbot, E. Bernard, J.P. Maurel, J.F. Faucon, J. Dufourcq, Melittin-phospholipid interactions: binding of the mono- and tetrameric form of this peptide, and perturbations of the thermotropic properties of bilayers, Toxicon 20 (1982) 199–202.
[23] J. Lauterwein, C. Bösch, L.R. Brown, K. Wüthrich, Physicochemical studies of the protein–lipid interactions in melittin-containing micelles, Biochimica et Biophysica Acta 556 (1979) 244–264.
[24] A.M. Batenburg, J.H. van Esch, B. de Kruijff, Melittin-induced changes of the macroscopic structure of phosphatidylethanolamines, Biochemistry 27 (1988) 2324–2331.
[25] A.M. Batenburg, J.C. Hibbeln, B. de Kruijff, Lipid specific penetration of melittin into phospholipid model membranes, Biochimica et Biophysica Acta 903 (1987) 142–154.
[26] A.M. Batenburg, J.H. van Esch, A.J. Verkleij, J. Leunissen- Bijvelt, B. de Kruijff, Interaction of melittin with negatively charged phospholipids: consequences for lipid organization, FEBS Letters 223 (1987) 148–154.
[27] G. Beschiaschvili, J. Seelig, Melittin binding to a mixed phosphatidyl-glycerol/phosphatidylcholine membranes, Biochemistry 29 (1990) 52–58.
[28] J.H. Kleinschmidt, J.E. Mahaney, D.D. Thomas, D. Marsh, Interaction of bee venom melittin with zwitterionic and negatively charged phospholipid bilayers: a spin-label electron spin resonance study, Biophysical Journal 72 (1997) 767–778.
[29] A.K. Ghosh, R. Rukmini, A. Chattopadhyay, Modulation of tryptophan in membrane-bound melittin by negatively charged phospholipids: implications in membrane organization and function, Biochemistry 36 (1997) 14291–14305.
[30] T. Benachir, M. Lafleur, Study of vesicle leakage induced by melittin, Biochimica et Biophysica Acta 1235 (1995) 452–460.
[31] M. Monette, M. Lafleur, Modulation of melittin induced lysis by surface-charge density of membranes, Biophysical Journal 68 (1995) 187–195.
[32] D.K. Hincha, J.H. Crowe, The lytic activity of the bee venom peptide melittin is strongly reduced by the presence of negatively charged phospholipids or chloroplast galactolipids in the membranes of phosphatidylcholine large unilamellar vesicles, Biochimica et Biophysica Acta 1284 (1996) 162–170.
[33] R.W. Ledeen, R.K. Yu, Gangliosides: structure, isolation, and analysis, Methods in Enzymology 83 (1982) 139–191.
[34] A. Gayen, C. Chatterjee, C. Mukhopadhyay, GM1-induced structural changes of bovine serum albumin after chemical and thermal disruption of the secondary structure: a spectroscopic comparison, Biomacromolecules 9 (2008) 974–983.
[35] S. Hakomori, Glycosphingolipids in cellular interaction, differentiation and oncogenesis, Annual Review of Biochemistry 50 (1981) 733–764.
[36] S. Hakomari, Bifunctional role of glycosphingolipids. Modulators for transmembrane signaling and mediators for cellular interactions, Journal of Biological Chemistry 265 (1990) 18713–18716.
[37] C.B. Zeller, R.B. Marchase, Gangliosides as modulators of cell function, American Journal of Physiology 262 (1992) C1341–C1355.
[38] S. Hakomari, Structure and function of sphingoglycolipids in transmembrane signaling and cell–cell interaction, Biochemical Society Transactions 21 (1993) 583–595.
[39] K. Simons, E. Ikonen, Functional rafts in cell membranes, Nature 387 (1997) 569–572.
[40] P. Doherty, S.V. Ashton, S.D. Skaper, A. Leon, F.S. Walsh, Ganglioside modulation of neural cell adhesion molecule and N-cadherin-dependent neurite outgrowth, The Journal of Cell Biology 117 (1992) 1093–1099.
[41] L.J. Wang, R. Colella, G. Yorke, F.J. Roisen, The ganglioside GM1 enhances microtubule networks and changes the morphology of neuro-2a cells *in vitro* by altering the distribution of MAP2, Experimental Neurology 139 (1996) 1–11.
[42] A. Sachinidis, R. Kraus, C. Seul, M.K. Meyer zu Brickwedde, K. Schulte, Y. Ko, J. Hoppe, H. Vetter, Gangliosides GM1, GM2 and GM3 inhibit platelet-derived

growth factor-induced signaling transduction pathway in vascular smooth muscle cells by different mechanisms, European Journal of Cell Biology 71 (1996) 79–88.
[43] T. Mutoh, A. Tokuda, T. Miyadai, M. Hamaguchi, N. Fujiki, Ganglioside GM1 binds to the Trk protein and regulates receptor function, Proceedings of the National Academy of Sciences of the United States of America 92 (1995) 5087–5091.
[44] L. Eidels, R.L. Proia, D.A. Hart, Membrane receptors for bacterial toxins, Microbiological Reviews 47 (1983) 596–620.
[45] P. Cohen, S. van Heyningen, Molecular Action of Toxins and Viruses, Elsevier, New York, 1982. 169–190.
[46] E.A. Merritt, S. Sarfaty, F. van den Akker, C. L'Hoir, J.A. Martial, W.J. Hol, Crystal structure of cholera toxin B-pentamer bound to receptor GM1 pentasaccharide, Protein Science 3 (1994) 166–175.
[47] a F. Superti, G. Donelli, Gangliosides as binding sites in SA-11 rotavirus infection of LLC-MK2 cells, Journal of General Virology 72 (1991) 2467–2474;
b Y. Miyazaki, M. Aoki, Y. Yano, K. Matsuzaki, Interaction of antimicrobial peptide Magainin 2 with gangliosides as a target for human cell binding, Biochemistry 51 (2012) 10229–10235;
c K.J. Glover, J.A. Whiles, G. Wu, N.-J. Yu, R. Deems, J.O. Struppe, R.E. Stark, E.A. Komives, R.R. Vold, Structural evaluation of phospholipid bicelles for solution-state studies of membrane-associated biomolecules, Biophysical Journal 81 (2001) 2163–2171.
[48] A. Gayen, S.K. Goswami, C. Mukhopadhyay, NMR evidence of GM1-induced conformational change of Substance P using isotropic bicelles, Biochimica et Biophysica Acta 1808 (2011) 127–139.
[49] A. Gayen, C. Mukhopadhyay, Evidence for effect of GM1 on opioid peptide conformation: NMR study on leucine enkephalin in ganglioside-containing isotropic phospholipid bicelles, Langmuir 24 (2008) 5422–5432.
[50] M. Nilsson, The DOSY toolbox: a new tool for processing PFG NMR diffusion data, Journal of Magnetic Resonance 200 (2009) 296–302.
[51] J. Wang, J.R. Schnell, J.J. Chou, Amantadine partition and localization in phospholipid membrane: a solution NMR study, Biochemical and Biophysical Research Communications 324 (2004) 212–217.
[52] I. Marcotte, F. Separovic, M. Auger, S.M. Gagné, A multidimensional ^{1}H NMR investigation of the conformation of methionine-enkephalin in fast-tumbling bicelles, Biophysical Journal 86 (2004) 1587–1600.
[53] S. Gaemers, A. Bax, Morphology of three lyotropic liquid crystalline biological NMR media studied by translational diffusion anisotropy, Journal of the American Chemical Society 123 (2001) 12343–12352.
[54] C. Chatterjee, C. Mukhopadhyay, Binding and folding of melittin in the presence of ganglioside GM1 micelles, Journal of Biomolecular Structure and Dynamics 23 (2005) 183–192.
[55] A. Andersson, J. Almqvist, F. Hagn, L. Maler, Diffusion and dynamics of penetratin in different membrane mimicking media, Biochimica et Biophysica Acta 1661 (2004) 18–25.
[56] L. Donghan, K.F.A. Walter, A.-K. Brückner, C. Hilty, S. Becker, C. Griesinger, Bilayer in small bicelles revealed by lipid–protein interactions using NMR spectroscopy, Journal of the American Chemical Society 130 (2008) 13822–13823.
[57] C. Kang, C.R. Sanders, W.D. Van Horn, C.G. Vanoye, R.C. Welch, Structure of KCNE1 and implications for how it modulates the KCNQ1 potassium channel, Biochemistry 49 (2010) 653–655.
[58] U.L. Khatun, S.K. Goswami, C. Mukhopadhyay, Modulation of the neurotensin solution structure in the presence of ganglioside GM1 bicelle, Biophysical Chemistry 168–169 (2012) 48–59.
[59] T. Yamaguchi, T. Uno, Y. Uekusa, M. Yagi-Utsumi, K. Kato, Ganglioside embedding small bicelles for probing membrane-landing processes of intrinsically disordered proteins, Chemical Communications (Cambridge, England) 49 (2013) 1235–1237.
[60] G. Wiedman, K. Herman, P. Searson, W.C. Wimley, K. Hristova, The electrical response of bilayers to the bee venom toxin melittin: evidence for transient bilayer permeabilization, Biochimica et Biophysica Acta 1828 (2013) 1357–1364.
[61] U.L. Khatun, A. Gayen, C. Mukhopadhyay, Gangliosides containing different numbers of sialic acids affect the morphology and structural organization of isotropic phospholipid bicelles, Chemistry and Physics of Lipids 170-171 (2013) 8–18.